Letter

Probing vortical structures in heavy-ion collisions at RHIC-BES energies through helicity polarization

Cong Yi,[1,*] Xiang-Yu Wu,[2,†] Di-Lun Yang,[3,‡] Jian-Hua Gao,[4,§] Shi Pu,[1,‖] and Guang-You Qin[2,¶]
[1]*Department of Modern Physics, University of Science and Technology of China, Hefei, Anhui 230026*
[2]*Institute of Particle Physics and Key Laboratory of Quark and Lepton Physics (MOE), Central China Normal University, Wuhan, Hubei 430079*
[3]*Institute of Physics, Academia Sinica, Taipei 11529*
[4]*Shandong Provincial Key Laboratory of Optical Astronomy and Solar-Terrestrial Environment, Institute of Space Sciences, Shandong University, Weihai, Shandong 264209*

(Received 28 July 2023; accepted 21 November 2023; published 5 January 2024)

We investigate the azimuthal angle dependent local hydrodynamic helicity polarization of Λ hyperons, defined as the projection of the spin polarization vector along the directions of particle momenta, at BNL Relativistic Heavy Ion Collider beam energy scan energies by utilizing the relativistic $(3+1)$D CLVisc hydrodynamics framework with SMASH initial conditions. As opposed to local spin polarization at high energy collisions, our hydrodynamic simulations demonstrate that the azimuthal angle dependent helicity polarization induced by the kinetic vorticity dominates over other contributions at intermediate and low collision energies. Our findings provide an opportunity to probe the fine structure of local kinetic vorticity as a function of azimuthal angle at intermediate and low collision energies by mapping our predictions to the future measurements in experiments.

DOI: 10.1103/PhysRevC.109.L011901

Introduction. Spin, as a fundamental property of particles, plays a critical role in high-energy physics, e.g., proton spin puzzles (see recent reviews [1,2] and references therein). Recently, a major breakthrough related to the spin polarization in the relativistic heavy ion collisions has drawn widespread attentions. In noncentral heavy-ion collisions, two heavy nuclei are accelerated to nearly the speed of light and collide with each other. These collisions generates a large amount of orbital angular momentum, estimated to be on the order of $10^5\hbar$. Such huge orbital angular momentum will be partially converted into spin polarization of the hadrons by spin-orbit coupling proposed by the pioneer works [3–5]. The STAR collaboration at the BNL Relativistic Heavy-Ion Collider (RHIC) has measured the global polarization of Λ and $\overline{\Lambda}$ hyperons [6]. The results show that the vorticity of the quark-gluon plasma (QGP) generated in the collisions is as large as $\omega \approx 10^{22}$ s^{-1}, making it the fastest vortical system observed in nature to date. The global polarization has been well understood by various phenomenological models [7–26].

Interestingly, the polarization along the beam and out-of-plane directions, namely, the local spin polarization has been measured by STAR [27,28] and ALICE [29], and are investigated by many different models, e.g., the statistical methods [30–32], quantum kinetic theory [33–69], spin hydrodynamics [70–98], other effective theories [99–101], and phenomenological simulations [12,16,17,19,102–110]. It is found that the local spin polarization can be induced by various sources, including the thermal vorticity, shear viscous tensor, fluid acceleration, gradient of baryon chemical potential over temperature, and electromagnetic fields [20,56,100,101,111–117]. These studies have also been extended to low-energy collisions [19,20,23,118–126] and isobaric collisions [127], as well as to the discussion on the vortical smoke rings [128,129]. Despite the global polarization having provided insight into the kinetic or thermal vorticity as a function of collision energies, the fine structure of the vorticity, such as its dependence on the azimuthal angle, have not been fully explored. These information may not been accurately captured by the local spin polarization due to the considerable influence of other sources beyond the thermal vorticity. In this work, we extend our previous studies [130] and demonstrate that the helicity polarization can help us to probe the fine structure of kinetic vorticity in low-energy collisions.

Helicity polarization, defined as the projection of spin polarization vector onto the direction of the particles' momentum, is widely used for characterizing the spin polarization in high energy physics [131]. In many high-energy scattering processes, there are no preferred quantization directions for

*congyi@mail.ustc.edu.cn
†xiangyuwu@mails.ccnu.edu.cn
‡dlyang@gate.sinica.edu.tw
§gaojh@sdu.edu.cn
‖shipu@ustc.edu.cn
¶guangyou.qin@ccnu.edu.cn

spin, unlike the case of global polarization where the direction of the initial orbital angular momentum is naturally chosen as the quantization direction. In such cases, helicity is often preferred over spin to describe the spin polarization.

Back to the heavy ion collisions, the use of helicity polarization allows us to probe a distinct feature of the spin polarization for Λ and $\overline{\Lambda}$ hyperons [132,133]. As mentioned previously, it is challenging to distinguish the local polarization of Λ hyperons induced by different sources through the experimental measurements. Remarkably, our previous study [130] has found that the local helicity polarization induced by thermal vorticity dominates over other contributions at $\sqrt{s_{NN}} = 200$ GeV Au+Au collisions. We argue that helicity polarization induced by kinetic vorticity, as part of thermal vorticity, will play the crucial role to the total helicity polarization in the low-energy collisions. Consequently, we further proposed that this finding can be utilized to probe the local strength of kinetic vorticity as a function of azimuthal angle in low-energy collisions by measuring helicity polarization.

To verify our conjecture, we utilize the relativistic (3 + 1)D CLVisc hydrodynamics framework [23,134,135] to investigate the azimuthal angle dependence of hydrodynamic helicity polarization at RHIC beam energy scan (BES) energies in this work. We report the numerical simulation of hydrodynamic helicity polarization at $\sqrt{s_{NN}} = 7.7$, 19.6, 39 GeV Au+Au collisions with simulating many accelerated strongly interacting hadrons (SMASH) [136–142] initial condition. As anticipated, the helicity polarization induced by the kinetic vorticity is one order of magnitude larger than other contributions in low-energy collisions. This finding holds even when we choose a multiphase transport (AMPT) [143–146] initial conditions or different baryon diffusion coefficients. Our study presents an approach to investigate the structure of kinetic vorticity in low-energy heavy-ion collisions by connecting hydrodynamic simulations with the measurable helicity polarization. The finding can also provide a baseline for the investigation on local parity violation through the correlations of helicity polarization proposed by [132,133].

This paper is organized as follows. We next briefly, introduce the theoretical framework and hydrodynamical setup for the helicity polarization. We then present our numerical results of the helicity polarization at various collision energies, initial conditions, and baryon diffusion coefficients, and then summarize our findings. Throughout this work, we adopt the Minkowski metric $g_{\mu\nu} = \text{diag}\{+,-,-,-\}$ and the projector $\Delta^{\mu\nu} = g^{\mu\nu} - u^\mu u^\nu$ with u^μ being fluid velocity.

Theoretical and numerical framework. We follow Refs. [30,130,132,133] to introduce the theoretical framework for the helicity polarization in relativistic heavy ion collisions. The helicity polarization for a relativistic particle with mass m is defined as

$$S^h = \widehat{\mathbf{p}}\cdot\boldsymbol{S}(\mathbf{p}). \tag{1}$$

Here, we parametrize the momentum of an on-shell particle as $p^\mu = (\sqrt{|\mathbf{p}|^2+m^2}, \mathbf{p}) = (\sqrt{p_T^2+m^2}\cosh Y, p_T\cos\phi_p, p_T\sin\phi_p, \sqrt{p_T^2+m^2}\sinh Y)$, where p_T is the transverse momentum, Y is the momentum rapidity and ϕ_p is the azimuthal angle, $\widehat{\mathbf{p}} = \mathbf{p}/|\mathbf{p}|$ is the unit vector along the direction of momentum, and $\boldsymbol{S}(\mathbf{p})$ is the spatial component of the single-particle mean spin polarization vector $\mathcal{S}^\mu(p)$. The spin polarization vector $\mathcal{S}^\mu(p)$ for fermionic systems can be evaluated by using the modified Cooper-Frye formula [9,10,59,114], under the assumption of local thermal equilibrium,

$$\mathcal{S}^\mu(\mathrm{p}) = \frac{\int d\Sigma\cdot p\mathcal{J}_5^\mu(p,X)}{2m_\Lambda\int d\Sigma\cdot\mathcal{N}(p,X)}, \tag{2}$$

where $d\Sigma^\mu$ is the normal vector of the freeze-out hypersurface, m_Λ denotes the mass of Λ hyperons, and $\mathcal{J}_5^\mu(p,X)$ and $\mathcal{N}^\mu(p,X)$ stand for the axial-charge and number-density current in the phase space, respectively.

Inserting the $\mathcal{J}_5^\mu(p,X)$ obtained from chiral kinetic theory up to $\mathcal{O}(\hbar)$ [59] into the spin polarization vector $\mathcal{S}^\mu$, we derive the helicity polarization [23,114,130],

$$\begin{aligned} S^h_{\text{hydro}}(\mathbf{p}) = {}& S^h_{\text{thermal}}(\mathbf{p}) + S^h_{\text{shear}}(\mathbf{p}) + S^h_{\text{accT}}(\mathbf{p}) \\ &+ S^h_{\text{chemical}}(\mathbf{p}), \end{aligned} \tag{3}$$

where

$$\begin{aligned} S^h_{\text{thermal}}(\mathbf{p}) &= \int d\Sigma^\sigma F_\sigma p_0 \epsilon^{0ijk}\widehat{p}_i\partial_j\left(\frac{u_k}{T}\right), \\ S^h_{\text{shear}}(\mathbf{p}) &= -\int d\Sigma^\sigma F_\sigma \frac{\epsilon^{0ijk}\widehat{p}^i p_0}{(u\cdot p)T}(p^\sigma\pi_{\sigma j}u_k), \\ S^h_{\text{accT}}(\mathbf{p}) &= \int d\Sigma^\sigma F_\sigma \frac{\epsilon^{0ijk}\widehat{p}^i p_0 u_j}{T}\left[(u\cdot\partial)u_k + \frac{\partial_k T}{T}\right], \\ S^h_{\text{chemical}}(\mathbf{p}) &= -2\int d\Sigma^\sigma F_\sigma \frac{p_0\epsilon^{0ijk}\widehat{p}_i}{(u\cdot p)}\partial_j\left(\frac{\mu}{T}\right)u_k, \end{aligned} \tag{4}$$

stand for the contributions from thermal vorticity, the shear viscous tensor, the fluid acceleration minus the gradient of temperature T, the gradient of baryon chemical potential μ over temperature, respectively. Here, we introduce $\pi_{\sigma j} = \partial_\sigma u_j + \partial_j u_\sigma - u_\sigma(u\cdot\partial)u_j$ and $F^\mu = \hbar[8m_\Lambda\Phi(\mathbf{p})]^{-1}p^\mu f_{eq}(1-f_{eq})$, $\Phi(\mathbf{p}) = \int d\Sigma^\mu p_\mu f_{eq}$. We also assume that the system reaches the local thermal equilibrium for simplicity, i.e., we choose $f_{eq} = 1/[\exp[(p^\mu u_\mu - \mu)/T] + 1]$. For other decomposition of spin vector, we refer to Refs. [100,101,103,111–113]. For convenience, we further decompose helicity polarization induced by thermal vorticity S^h_{thermal} into two separate terms [130],

$$\begin{aligned} S^h_{\nabla T}(\mathbf{p}) &= \int d\Sigma^\sigma F_\sigma \frac{p_0}{T^2}\widehat{\mathbf{p}}\cdot(\mathbf{u}\times\nabla T), \\ S^h_{\omega}(\mathbf{p}) &= \int d\Sigma^\sigma F_\sigma \frac{p_0}{T}\widehat{\mathbf{p}}\cdot\boldsymbol{\omega}, \end{aligned} \tag{5}$$

denoting the polarization related to the gradient of temperature, and caused by the kinetic vorticity $\boldsymbol{\omega} = \nabla\times\mathbf{u}$, respectively. Later on, we will see that the above decomposition can improve our understanding of helicity polarization.

Since the electromagnetic fields generating by the collisions decay rapidly [147–155] and are negligible at the late stage, we omit the helicity polarization induced by electromagnetic fields for simplicity. In general, an axial chemical potential, characterising local parity violation, near the freeze-out hypersurface also contributes to the helicity polarization

[132,133]. However, the event-by-event averaged axial density or axial chemical potential is almost vanishing. We therefore exclude these contributions in the analysis of helicity polarization. We also notice that in the absence of the axial charge the system has the space reversal symmetry, which leads to $S^h_{\rm hydro}(Y,\phi_p) = -S^h_{\rm hydro}(-Y,\phi_p+\pi)$. More discussions on the properties of helicity polarization can be found in Refs. [130,132,133].

Similar to the local spin polarization in heavy ion collisions, e.g., see Refs. [19,20,23,113,130], we propose a possible physical observable followed Ref. [130]:

$$P_H(\phi_p) = \frac{2\int_{Y_{\min}}^{Y_{\max}} dY \int_{p_{T\min}}^{p_{T\max}} p_T dp_T [\Phi(\mathbf{p}) S^h_{\rm hydro}]}{\int_{Y_{\min}}^{Y_{\max}} dY \int_{p_{T\min}}^{p_{T\max}} p_T dp_T \Phi(\mathbf{p})}. \quad (6)$$

The prefactor 2 in the numerator comes from experimental measurement of local spin polarization, which is proportional to $\frac{1}{s}\mathcal{S}^\mu(\mathbf{p})$ with $s=\frac{1}{2}$ for the Λ hyperons. Note that the S^h defined in Eq. (1) is not a Lorentz scalar. In the current study, we define the polarization three-vector $\boldsymbol{\mathcal{S}}$ in Eq. (6) in the laboratory frame, while the one defined in the rest frame of Λ hyperons can easily be derived by the Lorentz transformation, $\boldsymbol{\mathcal{S}}' = \boldsymbol{\mathcal{S}} - \frac{(\mathbf{p}\cdot\boldsymbol{\mathcal{S}})\mathbf{p}}{E_\Lambda(E_\Lambda+m_\Lambda)}$ with E_Λ being the energy of Λ hyperons. Similarly, the helicity polarization can also be defined by $\boldsymbol{\mathcal{S}}'$, i.e., $\widehat{\mathbf{p}}\cdot\boldsymbol{\mathcal{S}}' = \frac{m_\Lambda}{E_\Lambda}\widehat{\mathbf{p}}\cdot\boldsymbol{\mathcal{S}} = \frac{m_\Lambda}{E_\Lambda}S^h$.

To investigate the helicity polarization originating from various sources, we utilize Eq. (3) to express P_H as the sum of four terms and further decompose the thermal-vorticity contribution in light of Eq. (5),

$$P_H^{\rm total} = P_H^{\rm thermal} + P_H^{\rm shear} + P_H^{\rm accT} + P_H^{\rm chemical}, \quad (7)$$

$$P_H^{\rm thermal} = P_H^{\omega} + P_H^{\nabla T}, \quad (8)$$

where the superscripts indicate the respective sources.

We utilize the $(3+1)$D CLVisc hydrodynamics [23,134,135] to simulate the evolution of the QGP at different collision energies. We employ the SMASH model [136–142] for initial conditions and adopt the NEOS-BQS equations of state [156,157]. Later on, we will also check the results from the AMPT initial model [143–146]. We have chosen the simulation parameters according to the studies [23,135], where the hydrodynamic model has been shown to successfully reproduce the pseudorapidity distribution of charged hadrons, as well as the transverse momentum spectra of protons, pions, and kaons measured in the experiments. We would like to emphasize that the final results for the spectra of mesons in low energy collisions are insensitive to a parameter C_B, which connects to a baryon diffusion coefficient $\kappa_B = \frac{C_B}{T} n[\frac{1}{3}\cot(\frac{\mu}{T}) - \frac{nT}{w}]$ with n being baryon number and w being enthalpy density [23,135]. We set $C_B = 0$ in most of our simulations unless explicitly stated otherwise. From the simulations, we obtain the profile of temperature, chemical potential, and fluid velocity at the chemical freeze-out hypersurface. By inputting these quantities into Eqs. (2), (3), (6), we derive the helicity polarization as a function of the azimuthal angle ϕ_p. The integration bounds for Eq. (6) are chosen as $p_T \in [0.5, 3]$ GeV and $Y \in [-1, 1]$. We take the mass of Λ hyperons, $m_\Lambda = 1.116$ GeV in Eq. (2), as well as the mass term in all $(u\cdot p)$ terms of Eq. (4).

Numerical results from hydrodynamics approach. We present the numerical results for helicity polarization $P_H(\phi_p)$ induced by various sources as a function of azimuthal angle in 20–50 % centrality at $\sqrt{s_{NN}} = 7.7, 19.6, 39$ GeV Au+Au collisions. Similar to Refs. [27–29], we also compute the first Fourier sine coefficient of the helicity polarization of Λ hyperons, $\langle P_H \sin\phi_p\rangle$, as a function of transverse momentum.

Let us start by discussing the impact of collision energy on helicity polarization. As the collision energy decreases, nuclear stopping effects become more prominent and the larger portion of orbital angular momenta of colliding nuclei is transferred to the remnants. This leads to an expected growth of the kinetic vorticity with decreasing collision energies, as has been suggested by previous studies [16,121,158,159]. The experimental measurement of global polarization agrees with this expectation, that is, the global polarization increases as the collision energy decreases [6]. Naturally, one may expect that the helicity polarization induced by kinetic vorticity also follows the same trend, which is clearly observed in Fig. 1.

Furthermore, another important observation from Fig. 1 is that the P_H^{ω} dominates at intermediate and low collision energies. Unlike the global spin polarization successfully mainly described by the contribution from thermal vorticity in global equilibrium satisfying the Killing condition [160], other corrections such as the shear viscous tensor, gradient of baryon chemical potential over temperature should be incorporated in local thermal equilibrium, which play an important role to the local spin polarization [20,23,112–115,125,126]. Based on our previous studies [23], the magnitude of local spin polarization along the out-of-plane direction for Λ hyperons induced by shear viscous tensor, fluid acceleration, and $\nabla(\mu/T)$ at intermediate and low collision energies is much smaller than that caused by thermal vorticity. This conclusion holds if we choose the mass of particles in Eqs. (2) and (4) as the mass for Λ hyperons. Naturally, we anticipate that the helicity polarization induced by the thermal or kinetic vorticity dominates over other contributions.

As an example, we examine the behavior of P_H in $\sqrt{s_{NN}} =$ 7.7 GeV Au+Au collisions to demonstrate the contributions from various sources, as shown in Fig. 2(a). We observe that the magnitude of P_H^{ω} is approximately 10 times greater than that induced by other sources, which is consistent with the above analysis for the corrections out of global equilibrium. Furthermore, we observe that the dependence of $\{P_H^{\rm chemical}, P_H^{\rm shear}\}$ or $\{P_H^{\rm accT}, P_H^{\nabla T}\}$ on ϕ_p resembles that of the sine or negative sine function, respectively. Eventually, $P_H^{\rm chemical}, P_H^{\rm shear}, P_H^{\rm accT}, P_H^{\nabla T}$ nearly cancel each other out, highlighting the dominant role of kinetic vorticity in helicity polarization.

A natural question that arises is whether the dominant role of kinetic vorticity in helicity polarization persists for different initial conditions or parameters. To verify it, we have studied the helicity polarization at 7.7 GeV Au+Au collisions as an example using the AMPT initial conditions in Fig. 2(b), and with a different baryon diffusion coefficient $C_B = 1.2$ [23,135] in Fig. 2(c). We find that, regardless of the implemented initial conditions or the value of the baryon diffusion coefficient C_B, P_H^{ω} is always significantly larger than the helicity polarization induced by other sources even though

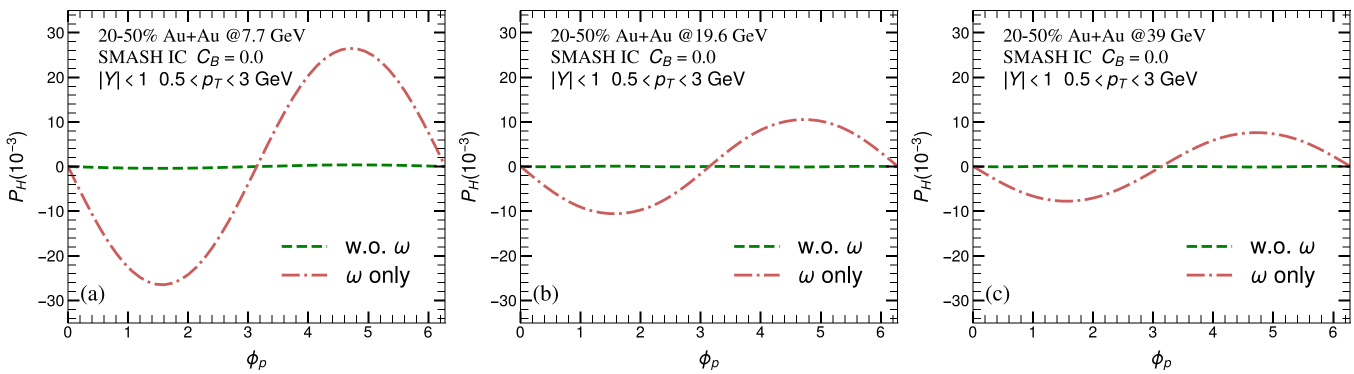

FIG. 1. Helicity polarization as a function of azimuthal angle ϕ_p in 20–50 % centrality at $\sqrt{s_{NN}} = 7.7$, 19.6, 39 GeV Au+Au collisions with SMASH initial condition. The red dash-dotted lines denote the helicity polarization induced by the kinetic vorticity ω only, i.e., P_H^{ω}. The green dashed lines represent the total helicity polarization excluding P_H^{ω}.

the magnitudes of helicity polarization from all sources including kinetic vorticity are together enhanced by a nonzero C_B. Therefore, our conclusion that P_H^{ω} dominates in P_H^{total} is independent of initial conditions or C_B. The helicity polarization induced by other sources, excluding the kinetic vorticity, also approximately cancel out with each other.

Another possible relevant observable in experiments is the first Fourier sine coefficient of the helicity polarization of Λ hyperons [27–29]. We plot $\langle P_H \sin\phi_p\rangle$ as a function of p_T in 20–50 % centrality at $\sqrt{s_{NN}} = 7.7$ GeV as an example in Fig. 3. We find that the magnitude of $\langle P_H \sin\phi_p\rangle$ increases with growing p_T. Moreover, we observe that helicity polarization induced by kinetic vorticity still dominates over other contributions, which is consistent with the results in Fig. 1.

As a remark, it is noteworthy that P_H^{ω} dominates the helicity polarization, especially in low energy collisions. Therefore, by mapping the hydrodynamic simulations to the helicity polarization measured in future experiments, one can extract the fine structure of kinetic vorticity.

Before ending this section, we would like to discuss the potential impact of two crucial approximations for the local spin polarization, namely, strange memory scenario [112] and isothermal equilibrium [113], on the helicity polarization. These two approximations are of great importance in delineating the local spin polarization of Λ hyperons at $\sqrt{s_{NN}} = 200$ GeV Au+Au collisions. However, in low-energy collisions, it is unclear whether the quark degrees of freedom are released from the hadrons in the fireball. Therefore, it is plausible to consider the helicity polarization of Λ hyperons rather than s quarks. We have also checked numerically that in strange memory scenarios, the helicity polarization induced by other effects, excluding kinetic vorticity, remains negligible and contributes only to a small percentage of the total helicity polarization. The sign of $\langle P_H \sin\phi_p\rangle$ remains unchanged in the strange memory scenarios. In the isothermal equilibrium, the temperature gradient near the chemical freeze-out hypersurface is assumed to be vanishing. We have numerically checked that even if we drop contributions from temperature gradient, the dominance of P_H^{ω} in the total helicity polarization still holds.

Furthermore, we draw a comparison between the local helicity polarization P_H and local spin polarization along the out-of-plane direction P^y. We emphasize that the helicity polarization P_H includes the contributions from the local spin

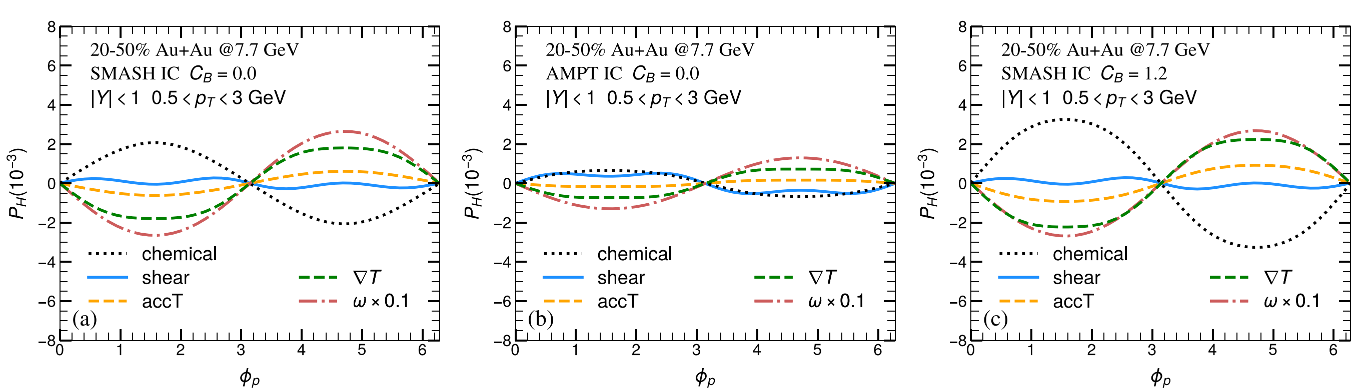

FIG. 2. (a) Helicity polarization induced by various sources in 20–50 % centrality at $\sqrt{s_{NN}} = 7.7$ GeV Au+Au collisions with SMASH initial condition. (b) The results were obtained using the same parameters as in Fig. 2(a) except for the initial condition given by AMPT model. (c) The results are obtained using the same parameters as in Fig. 2(a) except for $C_B = 1.2$. The shortened form “chemical”, “shear”, “accT”, “∇T”, and “$\omega \times 0.1$” stand for the P_H^{chemical}, P_H^{shear}, P_H^{accT}, $P_H^{\nabla T}$, and $0.1 \times P_H^{\omega}$, respectively.

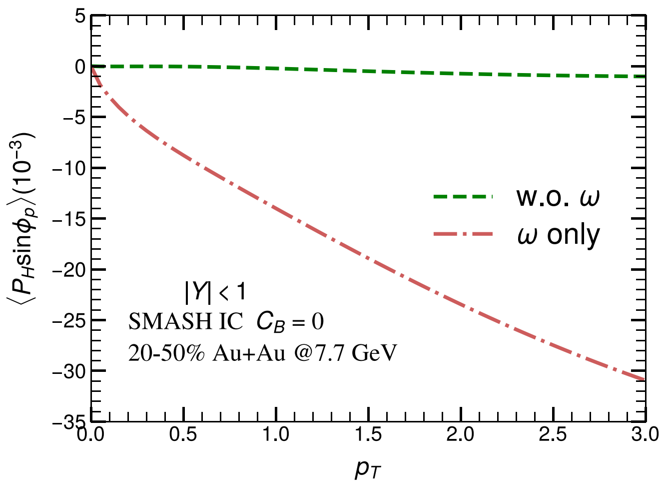

FIG. 3. The first Fourier sine coefficient of the helicity polarization as a function of p_T in 20 − 50% centrality at $\sqrt{s_{NN}} = 7.7$ GeV Au+Au collisions with SMASH initial condition. The same color assignments as in Fig. 1.

polarization along the out-of-plane, in-plane, and beam directions [cf. Eqs. (1) and (6)]. Consequently, P_H cannot be derived through a straightforward from P^y. Hence, the helicity polarization provides us additional information about the spin polarization for Λ hyperons. Another advantage for studying the helicity polarization is as follows. The hydrodynamic quantities, including thermal vorticity, shear viscous tensor, fluid acceleration, and others, can contribute to both local helicity polarization P_H and P^y. It is challenging to isolate the specific contribution of a single source through the P^y since some of these sources contribute to P^y at nearly the same order of magnitude [23]. In contrast, the azimuthal angle dependent helicity polarization P_H induced by the kinetic vorticity dominates. Therefore, it is straightforward for us to investigate helicity polarization from a phenomenological perspective and the relevant studies presents a new opportunity to probe the structure of kinetic vorticity.

Summary. We have studied the helicity polarization of Λ hyperons and its first Fourier sine coefficient at RHIC-BES energies and observed that the helicity polarization induced by kinetic vorticity P_H^{ω} dominates at intermediate and low collision energies. The helicity polarization led by other sources is one order of magnitude smaller than P_H^{ω} and their net contributions approximately cancel out. Furthermore, the dominance of P_H^{ω} remains unchanged by variations in initial conditions and baryon diffusion coefficient. Such a hierarchy for helicity polarization is also unchanged even when adopting the approximations of the strange memory scenarios and isothermal equilibrium in low-energy collisions.

Based on our results, we propose an approach to probe the fine structure of kinetic vorticity by linking hydrodynamic simulations to the measurements of helicity polarization in future low-energy nuclear collision experiments. On the other hand, at low-energy collisions, the helicity polarization provides a robust baseline for the equilibrium contribution to spin polarization. The sizable mismatch for comparing our predictions with future experimental measurements could reveal the potential role of nonequilibrium contributions from collisional effects or even more exotic sources to local spin polarization.

Acknowledgments. This work is supported in part by the National Key Research and Development Program of China under Contract No. 2022YFA1605500 and by the Chinese Academy of Sciences (CAS) under Grant No. YSBR-088. This work is also supported by National Natural Science Foundation of China (NSFC) under Grants No. 12075235, No. 12135011, No. 12225503, No. 12175123, No. 11890710, No. 11890711, No. 11890713, No. 11935007, and No. 11475104. D.-L.Y. was supported by National Science and Technology Council (Taiwan) under Grant No. MOST 110-2112-M-001-070-MY3 This work is also supported in part by Major Program of Natural Science Foundation of Shandong Province under Grant No. ZR2020ZD30.

[1] E. Leader and C. Lorcé, Phys. Rep. **541**, 163 (2014).
[2] M. Wakamatsu, Int. J. Mod. Phys. A **29**, 1430012 (2014).
[3] Z.-T. Liang and X.-N. Wang, Phys. Rev. Lett. **94**, 102301 (2005); **96**, 039901(E) (2006).
[4] Z.-T. Liang and X.-N. Wang, Phys. Lett. B **629**, 20 (2005).
[5] J.-H. Gao, S.-W. Chen, W.-t. Deng, Z.-T. Liang, Q. Wang, and X.-N. Wang, Phys. Rev. C **77**, 044902 (2008).
[6] L. Adamczyk *et al.* (STAR Collaboration), Nature (London) **548**, 62 (2017).
[7] F. Becattini and F. Piccinini, Ann. Phys. **323**, 2452 (2008).
[8] F. Becattini, F. Piccinini, and J. Rizzo, Phys. Rev. C **77**, 024906 (2008).
[9] F. Becattini, V. Chandra, L. Del Zanna, and E. Grossi, Ann. Phys. **338**, 32 (2013).
[10] R.-h. Fang, L.-g. Pang, Q. Wang, and X.-n. Wang, Phys. Rev. C **94**, 024904 (2016).
[11] I. Karpenko and F. Becattini, Eur. Phys. J. C **77**, 213 (2017).
[12] Y. Xie, D. Wang, and L. P. Csernai, Phys. Rev. C **95**, 031901(R) (2017).
[13] H. Li, L.-G. Pang, Q. Wang, and X.-L. Xia, Phys. Rev. C **96**, 054908 (2017).
[14] Y. Sun and C. M. Ko, Phys. Rev. C **96**, 024906 (2017).
[15] S. Shi, K. Li, and J. Liao, Phys. Lett. B **788**, 409 (2019).
[16] D.-X. Wei, W.-T. Deng, and X.-G. Huang, Phys. Rev. C **99**, 014905 (2019).
[17] X.-L. Xia, H. Li, Z.-B. Tang, and Q. Wang, Phys. Rev. C **98**, 024905 (2018).
[18] S. Shi, H. Zhang, D. Hou, and J. Liao, Phys. Rev. Lett. **125**, 242301 (2020).
[19] B. Fu, K. Xu, X.-G. Huang, and H. Song, Phys. Rev. C **103**, 024903 (2021).
[20] S. Ryu, V. Jupic, and C. Shen, Phys. Rev. C **104**, 054908 (2021).
[21] A. Lei, D. Wang, D.-M. Zhou, B.-H. Sa, and L. P. Csernai, Phys. Rev. C **104**, 054903 (2021).

[22] O. Vitiuk, L. V. Bravina, and E. E. Zabrodin, Phys. Lett. B **803**, 135298 (2020).
[23] X.-Y. Wu, C. Yi, G.-Y. Qin, and S. Pu, Phys. Rev. C **105**, 064909 (2022).
[24] V. E. Ambruş, J. High Energy Phys. 08 (2020) 016.
[25] V. E. Ambrus and M. N. Chernodub, Eur. Phys. J. C **83**, 111 (2023).
[26] V. E. Ambrus and M. N. Chernodub, Eur. Phys. J. C **82**, 1 (2020).
[27] T. Niida (Star Collaboration), Nucl. Phys. A **982**, 511 (2019).
[28] J. Adam *et al.* (STAR Collaboration), Phys. Rev. Lett. **123**, 132301 (2019).
[29] S. Acharya *et al.* (ALICE Collaboration), Phys. Rev. Lett. **128**, 172005 (2022).
[30] F. Becattini and I. Karpenko, Phys. Rev. Lett. **120**, 012302 (2018).
[31] F. Becattini, Rep. Prog. Phys. **85**, 122301 (2022).
[32] A. Palermo and F. Becattini, arXiv:2304.02276.
[33] J.-H. Gao and Z.-T. Liang, Phys. Rev. D **100**, 056021 (2019).
[34] N. Weickgenannt, X.-L. Sheng, E. Speranza, Q. Wang, and D. H. Rischke, Phys. Rev. D **100**, 056018 (2019).
[35] N. Weickgenannt, E. Speranza, X.-L. Sheng, Q. Wang, and D. H. Rischke, Phys. Rev. Lett. **127**, 052301 (2020).
[36] K. Hattori, Y. Hidaka, and D.-L. Yang, Phys. Rev. D **100**, 096011 (2019).
[37] Z. Wang, X. Guo, S. Shi, and P. Zhuang, Phys. Rev. D **100**, 014015 (2019).
[38] D.-L. Yang, K. Hattori, and Y. Hidaka, J. High Energy Phys. 07 (2020) 070.
[39] N. Weickgenannt, X.-L. Sheng, E. Speranza, Q. Wang, and D. H. Rischke, Nucl. Phys. A **1005**, 121963 (2021).
[40] S. Li and H.-U. Yee, Phys. Rev. D **100**, 056022 (2019).
[41] Y.-C. Liu, K. Mameda, and X.-G. Huang, Chin. Phys. C **44**, 094101 (2020).
[42] N. Weickgenannt, E. Speranza, X.-L. Sheng, Q. Wang, and D. H. Rischke, Phys. Rev. D **104**, 016022 (2021).
[43] Z. Wang and P. Zhuang, arXiv:2105.00915.
[44] X.-L. Sheng, N. Weickgenannt, E. Speranza, D. H. Rischke, and Q. Wang, Phys. Rev. D **104**, 016029 (2021).
[45] A. Huang, S. Shi, X. Zhu, L. He, J. Liao, and P. Zhuang, Phys. Rev. D **103**, 056025 (2021).
[46] Z. Wang, X. Guo, S. Shi, and P. Zhuang, Nucl. Phys. A **1005**, 121976 (2021).
[47] M. A. Stephanov and Y. Yin, Phys. Rev. Lett. **109**, 162001 (2012).
[48] D. T. Son and N. Yamamoto, Phys. Rev. D **87**, 085016 (2013).
[49] J.-H. Gao, Z.-T. Liang, S. Pu, Q. Wang, and X.-N. Wang, Phys. Rev. Lett. **109**, 232301 (2012).
[50] J.-W. Chen, S. Pu, Q. Wang, and X.-N. Wang, Phys. Rev. Lett. **110**, 262301 (2013).
[51] C. Manuel and J. M. Torres-Rincon, Phys. Rev. D **89**, 096002 (2014).
[52] C. Manuel and J. M. Torres-Rincon, Phys. Rev. D **90**, 076007 (2014).
[53] J.-Y. Chen, D. T. Son, M. A. Stephanov, H.-U. Yee, and Y. Yin, Phys. Rev. Lett. **113**, 182302 (2014).
[54] J.-Y. Chen, D. T. Son, and M. A. Stephanov, Phys. Rev. Lett. **115**, 021601 (2015).
[55] Y. Hidaka, S. Pu, and D.-L. Yang, Phys. Rev. D **95**, 091901(R) (2017).
[56] Y. Hidaka, S. Pu, and D.-L. Yang, Phys. Rev. D **97**, 016004 (2018).
[57] N. Mueller and R. Venugopalan, Phys. Rev. D **97**, 051901(R) (2018).
[58] Y. Hidaka and D.-L. Yang, Phys. Rev. D **98**, 016012 (2018).
[59] Y. Hidaka, S. Pu, and D.-L. Yang, Nucl. Phys. A **982**, 547 (2019).
[60] J.-H. Gao, Z.-T. Liang, Q. Wang, and X.-N. Wang, Phys. Rev. D **98**, 036019 (2018).
[61] A. Huang, S. Shi, Y. Jiang, J. Liao, and P. Zhuang, Phys. Rev. D **98**, 036010 (2018).
[62] Y.-C. Liu, L.-L. Gao, K. Mameda, and X.-G. Huang, Phys. Rev. D **99**, 085014 (2019).
[63] S. Lin and A. Shukla, J. High Energy Phys. 06 (2019) 060.
[64] S. Lin and L. Yang, Phys. Rev. D **101**, 034006 (2020).
[65] N. Yamamoto and D.-L. Yang, Astrophys. J. **895**, 56 (2020).
[66] J.-H. Gao, G.-L. Ma, S. Pu, and Q. Wang, Nucl. Sci. Tech. **31**, 90 (2020).
[67] J.-H. Gao, Z.-T. Liang, and Q. Wang, Int. J. Mod. Phys. A **36**, 2130001 (2021).
[68] Y. Hidaka, S. Pu, Q. Wang, and D.-L. Yang, Prog. Part. Nucl. Phys. **127**, 103989 (2022).
[69] S. Fang, S. Pu, and D.-L. Yang, Phys. Rev. D **106**, 016002 (2022).
[70] K. Hattori, M. Hongo, X.-G. Huang, M. Matsuo, and H. Taya, Phys. Lett. B **795**, 100 (2019).
[71] K. Fukushima and S. Pu, Lect. Notes Phys. **987**, 381 (2021).
[72] K. Fukushima and S. Pu, Phys. Lett. B **817**, 136346 (2021).
[73] S. Li, M. A. Stephanov, and H.-U. Yee, Phys. Rev. Lett. **127**, 082302 (2021).
[74] D. She, A. Huang, D. Hou, and J. Liao, Sci. Bull. **67**, 2265 (2021).
[75] D. Montenegro, L. Tinti, and G. Torrieri, Phys. Rev. D **96**, 076016 (2017).
[76] D. Montenegro, L. Tinti, and G. Torrieri, Phys. Rev. D **96**, 056012 (2017); **96**, 079901(E) (2017).
[77] W. Florkowski, B. Friman, A. Jaiswal, and E. Speranza, Phys. Rev. C **97**, 041901(R) (2018).
[78] W. Florkowski, E. Speranza, and F. Becattini, Acta Phys. Pol. B **49**, 1409 (2018).
[79] F. Becattini, W. Florkowski, and E. Speranza, Phys. Lett. B **789**, 419 (2019).
[80] W. Florkowski, R. Ryblewski, and A. Kumar, Prog. Part. Nucl. Phys. **108**, 103709 (2019).
[81] D.-L. Yang, Phys. Rev. D **98**, 076019 (2018).
[82] S. Bhadury, W. Florkowski, A. Jaiswal, A. Kumar, and R. Ryblewski, Phys. Lett. B **814**, 136096 (2021).
[83] S. Shi, C. Gale, and S. Jeon, Nucl. Phys. A **1005**, 121949 (2021).
[84] A. D. Gallegos, U. Gürsoy, and A. Yarom, Sci. Post Phys. **11**, 041 (2021).
[85] M. Hongo, X.-G. Huang, M. Kaminski, M. Stephanov, and H.-U. Yee, J. High Energy Phys. 11 (2021) 150.
[86] W. Florkowski, B. Friman, A. Jaiswal, R. Ryblewski, and E. Speranza, Phys. Rev. D **97**, 116017 (2018).
[87] W. Florkowski, A. Kumar, and R. Ryblewski, Phys. Rev. C **98**, 044906 (2018).
[88] W. Florkowski, A. Kumar, R. Ryblewski, and R. Singh, Phys. Rev. C **99**, 044910 (2019).

[89] W. Florkowski, A. Kumar, A. Mazeliauskas, and R. Ryblewski, Phys. Rev. C **100**, 054907 (2019).
[90] S. Bhadury, W. Florkowski, A. Jaiswal, A. Kumar, and R. Ryblewski, Phys. Rev. D **103**, 014030 (2021).
[91] S. Shi, C. Gale, and S. Jeon, Phys. Rev. C **103**, 044906 (2021).
[92] R. Singh, G. Sophys, and R. Ryblewski, Phys. Rev. D **103**, 074024 (2021).
[93] D.-L. Wang, S. Fang, and S. Pu, Phys. Rev. D **104**, 114043 (2021).
[94] Y.-C. Liu and X.-G. Huang, Nucl. Sci. Tech. **31**, 56 (2020).
[95] H.-H. Peng, J.-J. Zhang, X.-L. Sheng, and Q. Wang, arXiv:2107.00448.
[96] W. Florkowski, R. Ryblewski, R. Singh, and G. Sophys, Phys. Rev. D **105**, 054007 (2022).
[97] P. Copinger and S. Pu, Phys. Rev. D **105**, 116014 (2022).
[98] D.-L. Wang, X.-Q. Xie, S. Fang, and S. Pu, Phys. Rev. D **105**, 114050 (2022).
[99] J.-j. Zhang, R.-h. Fang, Q. Wang, and X.-N. Wang, Phys. Rev. C **100**, 064904 (2019).
[100] S. Y. F. Liu and Y. Yin, Phys. Rev. D **104**, 054043 (2021).
[101] S. Y. F. Liu and Y. Yin, J. High Energy Phys. 07 (2021) 188.
[102] S. A. Voloshin, EPJ Web Conf. **171**, 07002 (2018).
[103] S. Y. F. Liu, Y. Sun, and C. M. Ko, Phys. Rev. Lett. **125**, 062301 (2020).
[104] H.-Z. Wu, L.-G. Pang, X.-G. Huang, and Q. Wang, Nucl. Phys. A **1005**, 121831 (2021).
[105] H.-Z. Wu, L.-G. Pang, X.-G. Huang, and Q. Wang, Phys. Rev. Res. **1**, 033058 (2019).
[106] X.-L. Xia, H. Li, X.-G. Huang, and H. Z. Huang, Phys. Rev. C **100**, 014913 (2019).
[107] F. Becattini, G. Cao, and E. Speranza, Eur. Phys. J. C **79**, 741 (2019).
[108] H. Li, X.-L. Xia, X.-G. Huang, and H. Z. Huang, EPJ Web Conf. **259**, 11017 (2022).
[109] W. Florkowski, A. Kumar, A. Mazeliauskas, and R. Ryblewski, Phys. Rev. C **105**, 064901 (2022).
[110] Y. Sun, Z. Zhang, C. M. Ko, and W. Zhao, Phys. Rev. C **105**, 034911 (2022).
[111] F. Becattini, M. Buzzegoli, and A. Palermo, Phys. Lett. B **820**, 136519 (2021).
[112] B. Fu, S. Y. F. Liu, L. Pang, H. Song, and Y. Yin, Phys. Rev. Lett. **127**, 142301 (2021).
[113] F. Becattini, M. Buzzegoli, A. Palermo, G. Inghirami, and I. Karpenko, Phys. Rev. Lett. **127**, 272302 (2021).
[114] C. Yi, S. Pu, and D.-L. Yang, Phys. Rev. C **104**, 064901 (2021).
[115] S. Alzhrani, S. Ryu, and C. Shen, Phys. Rev. C **106**, 014905 (2022).
[116] M. Buzzegoli, F. Becattini, G. Inghirami, I. Karpenko, and A. Palermo, Acta Phys. Pol. B: Proc. Suppl. **16**, 39 (2023).
[117] A. Palermo, F. Becattini, M. Buzzegoli, G. Inghirami, and I. Karpenko, EPJ Web Conf. **276**, 01026 (2023).
[118] F. K. for HADES Collaboration, Talk Given at Strangeness Quark Matter 2021, online, May 17–22, 2021; Talk Given at the 6th International Conference on Chirality, Vorticity and Magnetic Field in HIC, online, Nov. 1–5, 2021.
[119] M. S. Abdallah *et al.* (STAR Collaboration), Phys. Rev. C **104**, L061901 (2021).
[120] Y. B. Ivanov, V. D. Toneev, and A. A. Soldatov, Phys. Rev. C **100**, 014908 (2019).
[121] X.-G. Deng, X.-G. Huang, Y.-G. Ma, and S. Zhang, Phys. Rev. C **101**, 064908 (2020).
[122] Y. Guo, J. Liao, E. Wang, H. Xing, and H. Zhang, Phys. Rev. C **104**, L041902 (2021).
[123] A. Ayala, I. Domínguez, I. Maldonado, and M. E. Tejeda-Yeomans, Phys. Rev. C **105**, 034907 (2022).
[124] X.-G. Deng, X.-G. Huang, and Y.-G. Ma, Phys. Lett. B **835**, 137560 (2022).
[125] B. Fu, L. Pang, H. Song, and Y. Yin, arXiv:2201.12970.
[126] B. Fu, L. Pang, H. Song, and Y. Yin, arXiv:2208.00430.
[127] M. I. Abdulhamid *et al.* (STAR Collaboration), Phys. Rev. Lett. **131**, 202301 (2023).
[128] M. A. Lisa, J. G. P. Barbon, D. D. Chinellato, W. M. Serenone, C. Shen, J. Takahashi, and G. Torrieri, Phys. Rev. C **104**, L011901 (2021).
[129] W. M. Serenone *et al.*, Phys. Lett. B **820**, 136500 (2021).
[130] C. Yi, S. Pu, J.-H. Gao, and D.-L. Yang, Phys. Rev. C **105**, 044911 (2022).
[131] E. Leader, *Spin in Particle Physics*, Cambridge Monographs on Particle Physics, Nuclear Physics and Cosmology (Cambridge University Press, Cambridge, 2001).
[132] F. Becattini, M. Buzzegoli, A. Palermo, and G. Prokhorov, Phys. Lett. B **822**, 136706 (2021).
[133] J.-H. Gao, Phys. Rev. D **104**, 076016 (2021).
[134] L. Pang, Q. Wang, and X.-N. Wang, Phys. Rev. C **86**, 024911 (2012).
[135] X.-Y. Wu, G.-Y. Qin, L.-G. Pang, and X.-N. Wang, Phys. Rev. C **105**, 034909 (2022).
[136] J. Weil *et al.*, Phys. Rev. C **94**, 054905 (2016).
[137] A. Schäfer, J. M. Torres-Rincon, J. Rothermel, N. Ehlert, C. Gale, and H. Elfner, Phys. Rev. D **99**, 114021 (2019).
[138] J. Mohs, S. Ryu, and H. Elfner, J. Phys. G: Nucl. Part. Phys. **47**, 065101 (2020).
[139] J. Hammelmann, A. Soto-Ontoso, M. Alvioli, H. Elfner, and M. Strikman, Phys. Rev. C **101**, 061901(R) (2020).
[140] J. Mohs, M. Ege, H. Elfner, and M. Mayer, Phys. Rev. C **105**, 034906 (2022).
[141] A. Schäfer *et al.*, Eur. Phys. J. A **58**, 230 (2022).
[142] G. Inghirami and H. Elfner, Eur. Phys. J. C **82**, 796 (2022).
[143] Z.-W. Lin, C. M. Ko, B.-A. Li, B. Zhang, and S. Pal, Phys. Rev. C **72**, 064901 (2005).
[144] X.-Y. Wu and G.-Y. Qin, arXiv:2109.03512.
[145] X.-Y. Wu, L.-G. Pang, G.-Y. Qin, and X.-N. Wang, Phys. Rev. C **98**, 024913 (2018).
[146] W. Zhao, H.-j. Xu, and H. Song, Eur. Phys. J. C **77**, 645 (2017).
[147] W.-T. Deng and X.-G. Huang, Phys. Rev. C **85**, 044907 (2012).
[148] V. Roy and S. Pu, Phys. Rev. C **92**, 064902 (2015).
[149] V. Roy, S. Pu, L. Rezzolla, and D. Rischke, Phys. Lett. B **750**, 45 (2015).
[150] S. Pu, V. Roy, L. Rezzolla, and D. H. Rischke, Phys. Rev. D **93**, 074022 (2016).
[151] S. Pu and D.-L. Yang, Phys. Rev. D **93**, 054042 (2016).
[152] G. Inghirami *et al.*, Eur. Phys. J. C **76**, 659 (2016).
[153] S. Shi, Y. Jiang, E. Lilleskov, and J. Liao, Ann. Phys. **394**, 50 (2018).
[154] I. Siddique, R. J. Wang, S. Pu, and Q. Wang, Phys. Rev. D **99**, 114029 (2019).
[155] H.-H. Peng, S. Wu, R.-j. Wang, D. She, and S. Pu, Phys. Rev. D **107**, 096010 (2023).

[156] A. Monnai, B. Schenke, and C. Shen, Phys. Rev. C **100**, 024907 (2019).
[157] A. Monnai, B. Schenke, and C. Shen, Int. J. Mod. Phys. A **36**, 2130007 (2021).
[158] W.-T. Deng and X.-G. Huang, Phys. Rev. C **93**, 064907 (2016).
[159] X.-G. Huang, Nucl. Phys. A **1005**, 121752 (2021).
[160] F. Becattini, Phys. Rev. Lett. **108**, 244502 (2012).